Angewandte Chemie
Eine Zeitschrift der Gesellschaft Deutscher Chemiker

Supporting Information

A New Type of Supramolecular Fluid Based on H_2O–Alkylammonium/Phosphonium Solutions

Carlos López-Bueno, Carlos Herreros-Lucas, Manuel Suárez-Rodríguez, Marius R. Bittermann, Alfredo Amigo, Sander Woutersen, María Giménez-López, and Francisco Rivadulla**

ange_202015800_sm_miscellaneous_information.pdf

Table of Contents

1. Experimental Procedures……2
2. Thermal conductivity of TtBABr solutions……2
3. Spectroscopic characterization of the solutions: IR and NMR……4
4. Characterization of other salts: TtBACl and TtBPBr……7
5. Electrochemistry with Cu electrodes……9

1. Experimental Procedures

Water solutions of tetrabuthylammonium bromide (TtBABr) and tetrabutyl phosphonium bromide (TtBPBr) were prepared by dissolving TtBABr (>99%) or TtBPBr (98%) from Sigma-Aldrich, in Mili-Q grade water. Similar reagents were used to prepare the TtBACl solutions. DSC measurements were carried out using a TA Instruments Q200 system. Adiabatic compressibility data were obtained from density and ultrasound velocity (~3 MHz) measurements recorded with an Anton Paar DSA 5000 calibrated with water and dry air. Specific heat was measured in a Setaram Micro DSC-III, also calibrated with water. Thermal conductivity measurements were performed at room temperature under ambient pressure, using the 3□ method, in a homemade setup as described in Ref.[35]. A small amount of solution (1 µL) was used for each measurement, to avoid the effect of convective flows. All measurements were repeated at least three times, for reproducibility. IR experiments were performed in a Perkin Spectrum Two FTIR spectrometer. 1 □l of liquid was placed between two CaF2 windows inserted in a liquid-N2 cryostat (DNI1704, Oxford Instruments). The experiments were performed in aqueous solutions of 4% D2O: H2O.
Bromiun-79 NMR spectra were measured in a 11.7 T Bruker Avance DRX-500 spectrometer equipped with a BBI probe. The spectra were acquired with the pulse-acquisition sequence (zg sequence of the Bruker library). The number of scans was 2048. The inter-scan delay (d1) was 0.1s. The acquisition time was 0.217s. The spectral window is centered at -100 ppm and covers a spectral width of 600 ppm. NMR samples were prepared in thin wall 5 mm NMR tubes. For deuterium lock and shimming a capillary containing D2O was inserted coaxially in the NMR tube. Raman spectra were measured under ambient conditions with a Renishaw Raman model InVia Reflex spectrometer with a laser wavelength of 514nm. Viscosity data was recorded with an Anton Paar SVM3000 Stabinger Viscosimeter.

Electrochemical experiments were carried out on a computer-controlled potentiostat (Autolab 201A) at room temperature using a conventional three-electrode in an aqueous solution. A Pt wire and an Ag/AgCl electrode were used as the counter and reference electrode, respectively. For investigating the role of TBA+ in the electrochemical oxidation of platinum nanoparticles, a glassy carbon electrode (GCE, 3mm diameter) was modified by drop casting a suspension of Pt/C in water, having a platinum loading of 14 µg cm−2. Prior to use, the working GCE was polished mechanically with aqueous slurries of alumina powder (0.05 µm), rinsed with Mill-Q water and acetone and allowed to dry under nitrogen. Cyclic voltammograms and chronoamperometry experiments were performed in hydrogen saturated conditions, both in 1.8m KBr and 1.8m TtBABr at scan rates of 50 mV s−1 between -0.6 V and 0.6 V. Pt/C (20 wt%, HiSPECTM 3000) was supplied by Alfa Aesar.
In the copper corrosion study, a Cu wire (0.064cm2) was used as a working electrode in the same three-electrode set-up. Cyclic voltammograms and chronoamperometry experiments were performed in nitrogen saturated conditions, both in 1.8m KCl and 1.8m TtBACl at scan rates of 50 mV s−1 between -1.5 V and 0.3 V and at 0,3V for a certain amount of time, respectively.

2. Thermal conductivity of TtBABr solutions.

To further support our interpretation of the thermal conductivity results we measured the κ of a $Mg(ClO_4)_2$ solution. This salt increases the viscosity of water, by as much as 30% at a 1 M concentration. However, Omta et al.[36] showed that this effect is due to an increase of the rotational dynamics of water molecules in the first solvation shells of the ions, while hydrogen-bond network in bulk water (outside the solvation shell) remains unaffected. We prepared a solution of $Mg(ClO_4)_2 \approx 1.85$ m, to reach a salt:water ratio = 1:30, as in the TtBABr 1.8 m solution. The IR spectra shown in Figure S2 confirms the presence of strong hydrogen bonds between the ClO_4^- ion and water molecules, observable as a high frequency shoulder at the -O-H stretching band of water.[36] However, in spite of this increase of viscosity, the thermal conductivity only decreases by 15%, compared to 50% in the TtBABr at a similar molecular ratio.

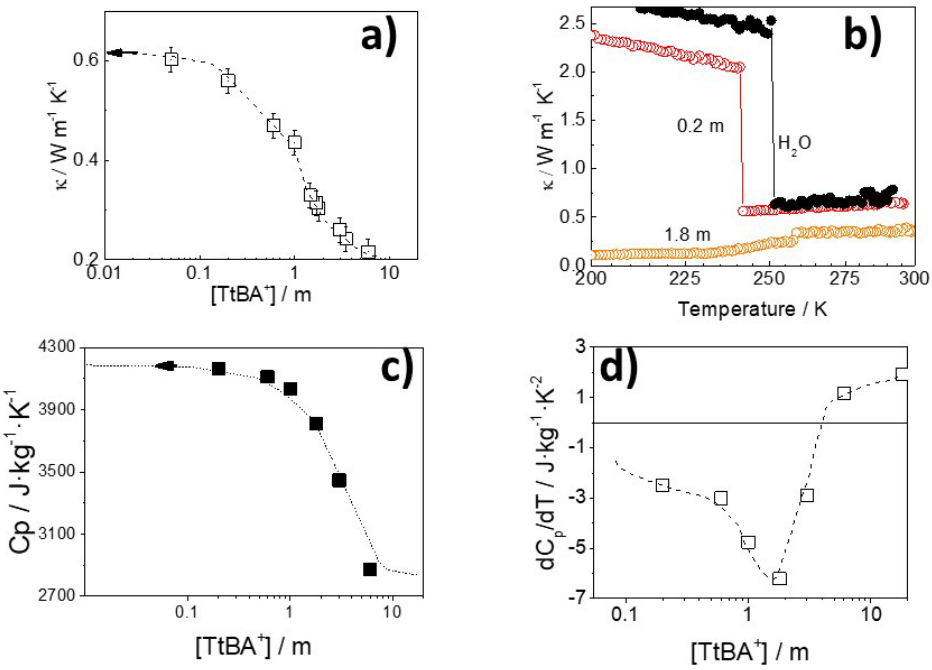

Figure S1. Room temperature thermal conductivity (a) and its temperature dependence (b) for different concentrations of TtBABr. In c) and d) we show the room temperature heat capacity and dC_p/dT, respectively, for different solutions. The arrows mark the value for pure water.

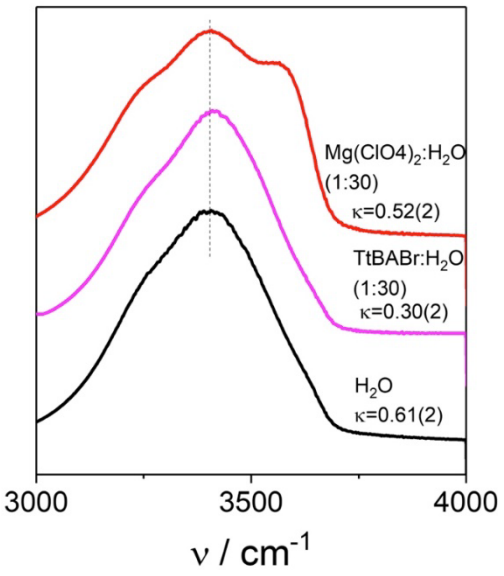

Figure S2. Comparison of the high frequency band (stretching of intramolecular O-H mode) in water, 1.8 m $TtBA^+$ solution (TtBA:water=1:30), and a water solution of $Mg(ClO_4)_2$. The concentration of ClO_4^- adjusted to reach a molecular ratio ClO_4^-:H_2O = 1:30, like in the TtBABr solution. The high frequency shoulder in the solution of $Mg(ClO_4)_2$ corresponds -O-H bounded to ClO_4^- ion. The thermal conductivity for each solution is indicated in W m^{-1} K^{-1}.

Assuming 4 water molecules coordinating each ClO_4^- ion, this makes 13% of them in a 1.8 m solution of perchlorate. If these water molecules contribute to the total thermal conductivity with 0.2 W/mK (a common value to other molecular liquids with no so strong H-bonds), and the remaining 87% as bulk water, with κ=0.6 W/mK, multiplying the molar fraction by its thermal conductivity gives a value for the solution of 0.54 W/mK, similar to the experimental value of 0.52 W/mK.
This result demonstrates that the dramatic reduction of the thermal conductivity of the solutions of TtBABr around 1.8 m is due to an effect over the majority of water molecules of the system.

The singularity of the tetrabutyl arrangement in the ammonium ion is demonstrated below. The comparison with shorter alkyl-chain salts shows that only the tetrabutylamonium shows a minimum around a range of concentrations with singular mechanical and thermodynamical properties, as described in the paper.

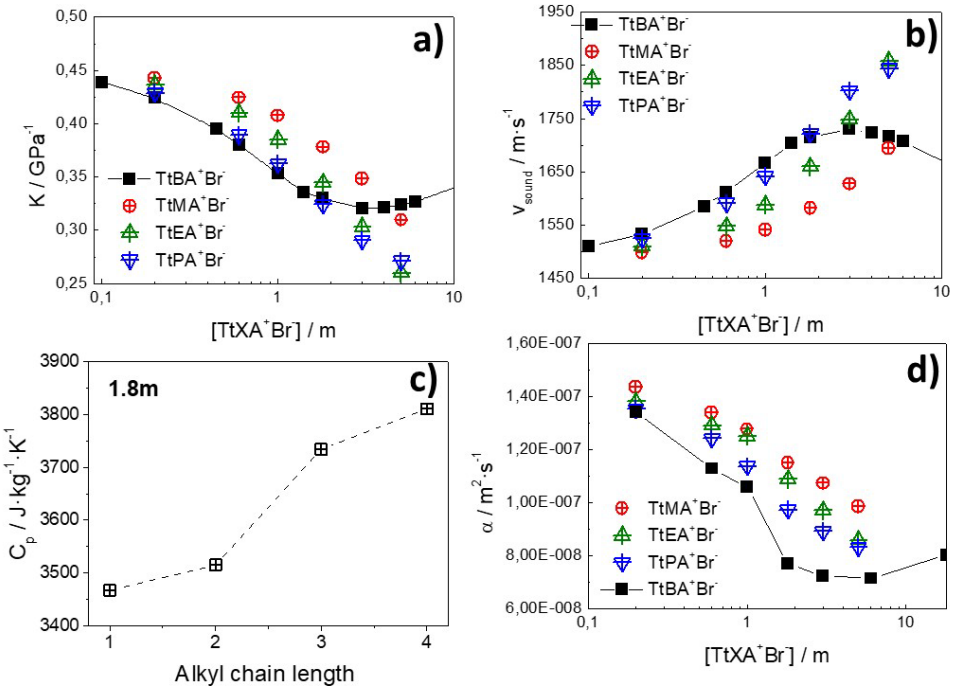

Figure S3. Room temperature compressibility (a), speed of sound (b) heat capacity (at 1.8 m) (c), and thermal diffusivity (d) for tetra methyl, ethyl, propyl and butyl- ammonium bromide in water. The minimum (maximum) in K and α (speed of sound) of the tetrabutylammounium salt around 1.8-3 m is not observed in shorter alkylammonium salts.

3. Spectroscopic characterization of the solutions: IR and NMR.

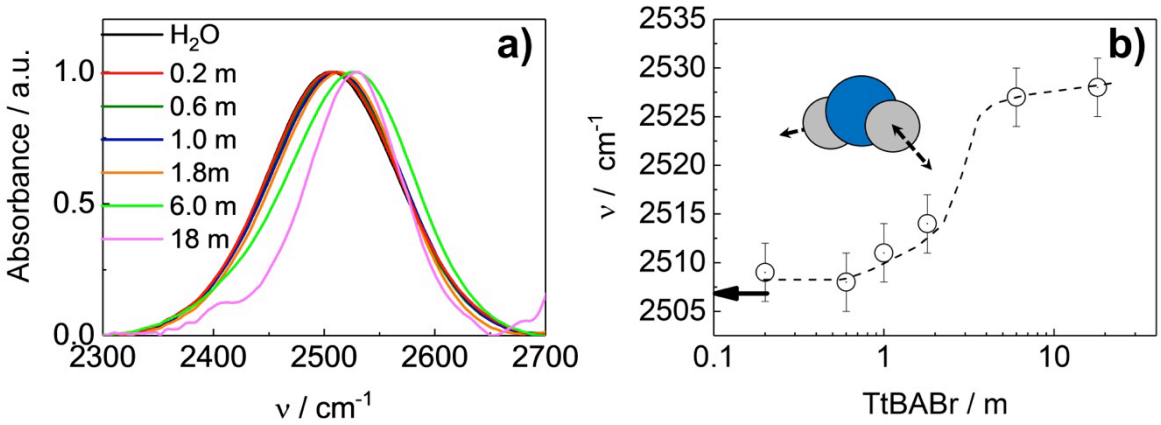

Figure S4. a) Room temperature IR spectra at different concentrations of TtBABr. b) Change in the frequency at the maximum absorption for different concentrations.

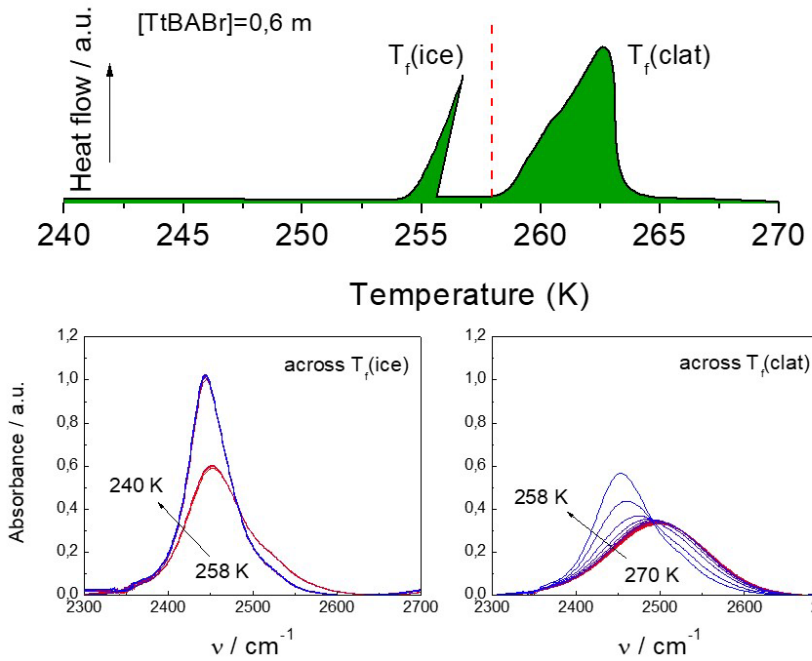
[TtBABr]=0,6 m
Heat flow / a.u.
T_f(ice)
T_f(clat)
240
245
250
255
260
265
270
Temperature (K)
Absorbance / a.u.
across T_f(ice)
240 K
258 K
across T_f(clat)
258 K
270 K
ν / cm^{-1}

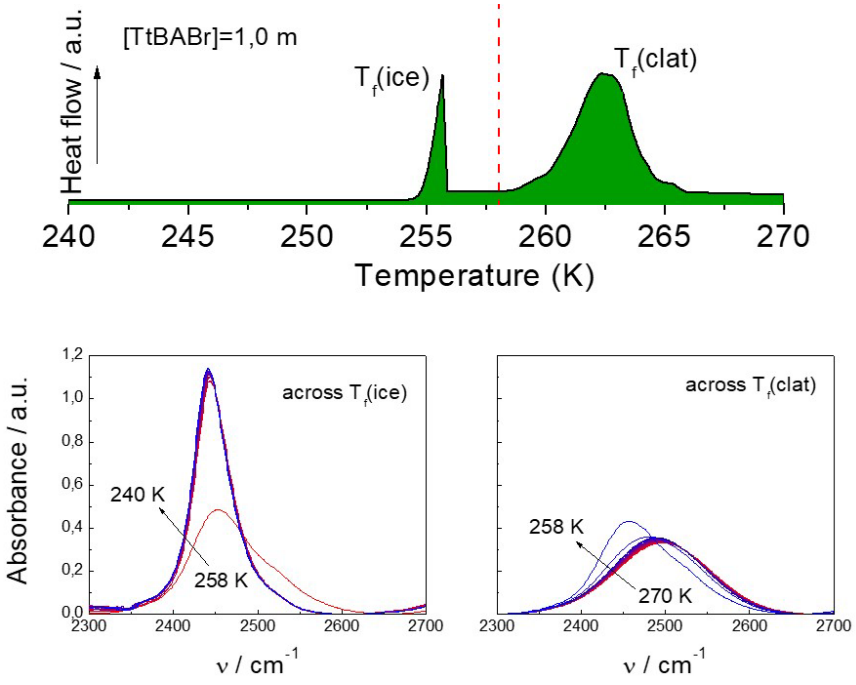
[TtBABr]=1,0 m
Heat flow / a.u.
T_f(ice)
T_f(clat)
240
245
250
255
260
265
270
Temperature (K)
Absorbance / a.u.
across T_f(ice)
240 K
258 K
across T_f(clat)
258 K
270 K
ν / cm^{-1}

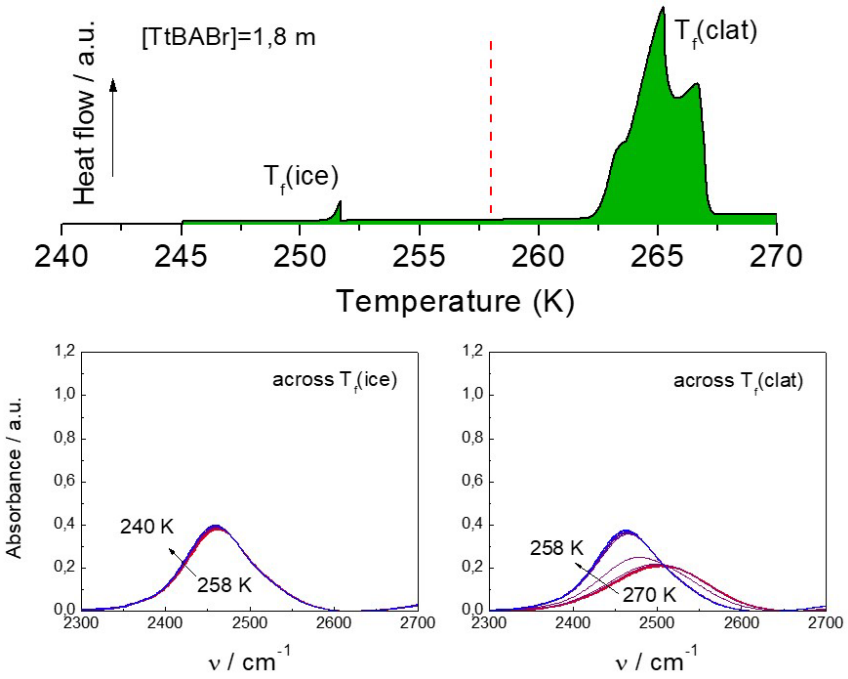

Figure S5. Comparison of calorimetric (DSC) and IR data across the temperature of formation of the clatrate, T_f(clat), and ice, T_f(ice), during cooling, for three different solutions, with [TtBABr]=0.6 m (top panel), 1.0 m (middle panel), 1.8 m (bottom panel). The IR spectra shows only a small change across T_f(clat), very similar in all solutions. A large change is observed across T_f(ice); whose contribution depends on the amount of free water in each solution. The same cooling rate of 2ºC/min was used in the DSC and IR scans. The same scale has been used in all plots for comparison among different samples.

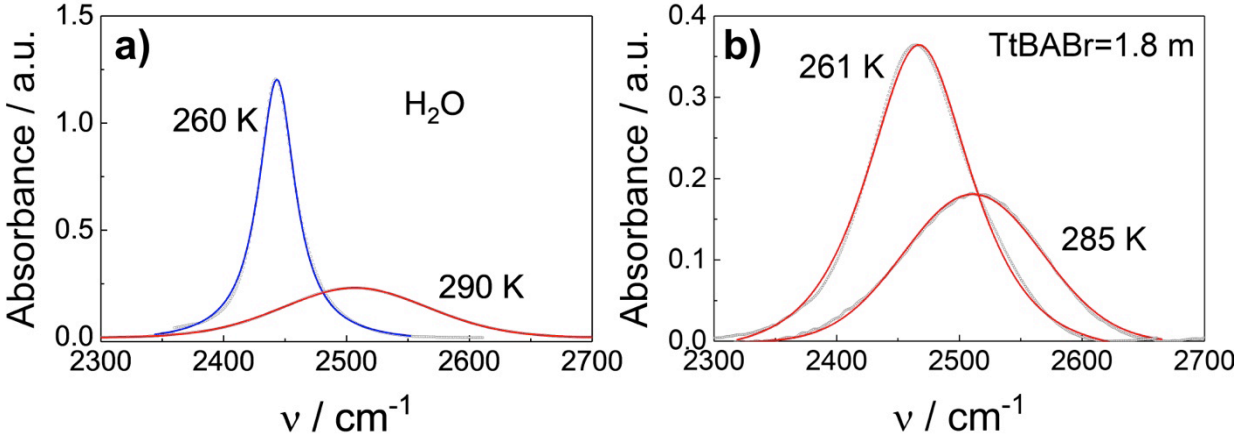

Figure S6. Fitting of experimental absorption (grey symbols) of pure water (a) and TtBABr 1.8 m (b) at room temperature and in the solid state at low temperature. Red/blue continuous lines represent the fitting to Gaussian and Lorentzian functions, respectively.

To study the possible role of an increasing viscosity of the TtBABr aqueous solutions in the ^{79}Br NMR line broadening, we calculated the expected change of the NMR linewidth using the Stokes-Einstein equation[37]: $\Delta H \propto 1/D = 6\pi\eta r/k_B T$, where η is the dynamic viscosity, r is the hydrodynamic radius, and T, the temperature. We also measured several 1.1m solutions of KBr in water-ethyleneglycol solutions of different concentration, to match the viscosities of the TtBABr solutions. The results are shown in Figure S7.
The increase of the linewidth of Br^- in water-ethyleneglycol matches nicely the predictions from Stokes-Eistein equation. However, the much larger broadening observed in the TtBABr is not compatible with a simple increase in the viscosity, supporting our hypothesis that Br^- is forming part of the cages in the liquid phase.

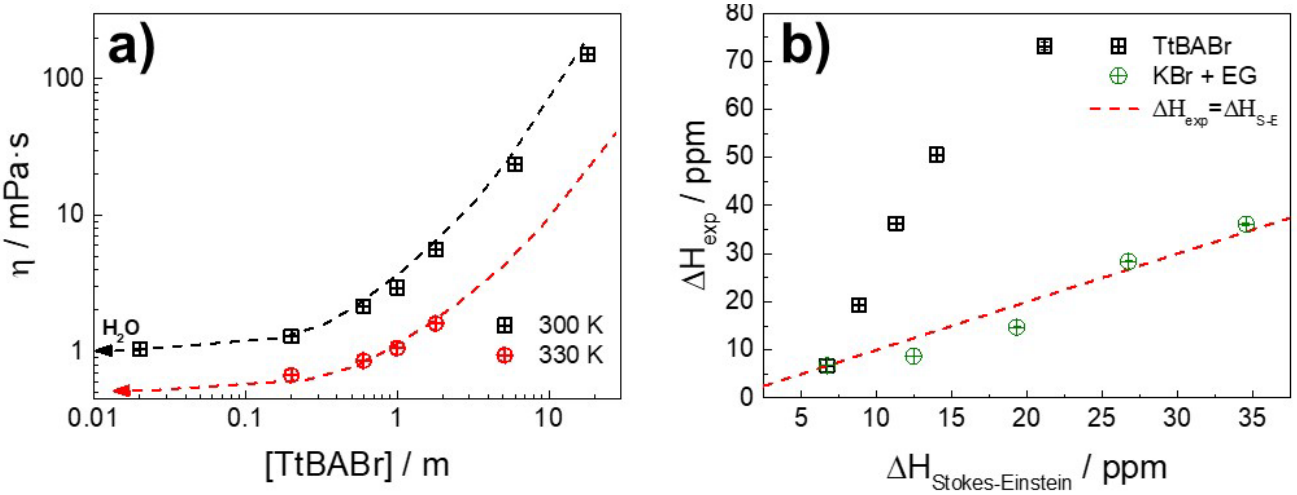

Figure S7. (a) Experimental values for the viscosity for different concentrations of TtBABr. (b) Comparison between the experimental ^{79}Br NMR linewidth (black squares) and the predicted by the Stokes-Einstein equation (red line), relative to the linewidth of a 1.1m KBr solution (green solid circle). The measurements were performed at 330K.
From the difference between the experimental linewidth and the contribution from the viscosity, we can calculate an effective hydrodynamic ratio of the Br^-:

Taking into account that Br^- in water has 6-7.4 water molecules in its hydration shell,[38] the size of the hydration sphere of Br^- in a 1.8 m solution of TtBABr is ≈7.8 times larger than in a KBr solution, compatible with the formation of large structures at room temperature.

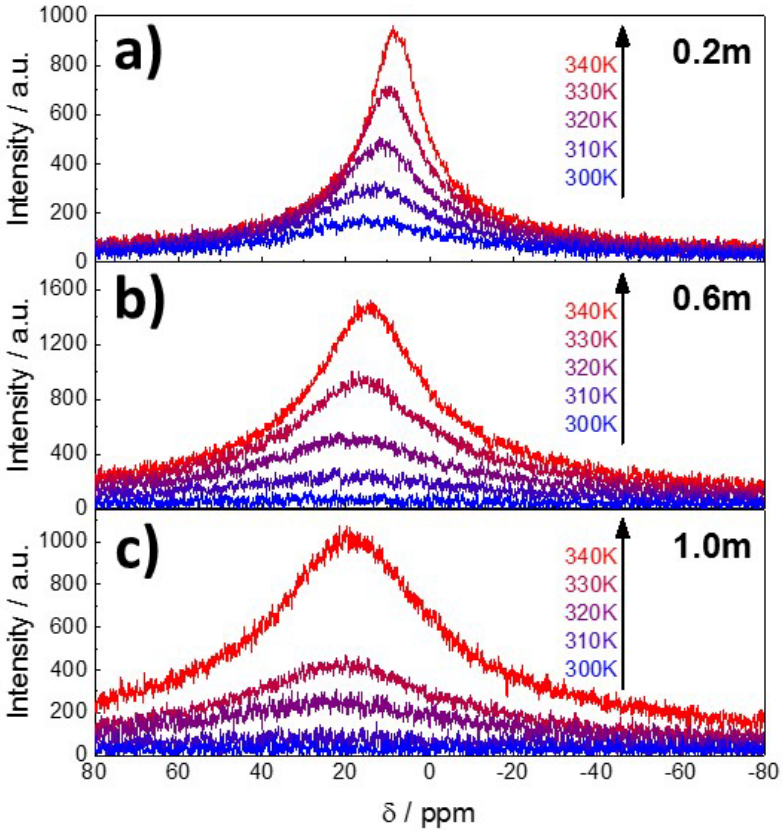

Figure S8. Temperature dependence of ^{79}Br for different concentrations of TtBABr. We observe the expected narrowing by increasing the temperature. It is noticeable that 0.2 m sample shows the peak even at room temperature. As in the solid state, where a specific water-salt ratio is needed to form the clathrate, similar ratios are needed in the liquid to form the supramolecular clathrate structures.

4. Characterization of other salts: TtBACl and TtBPBr.

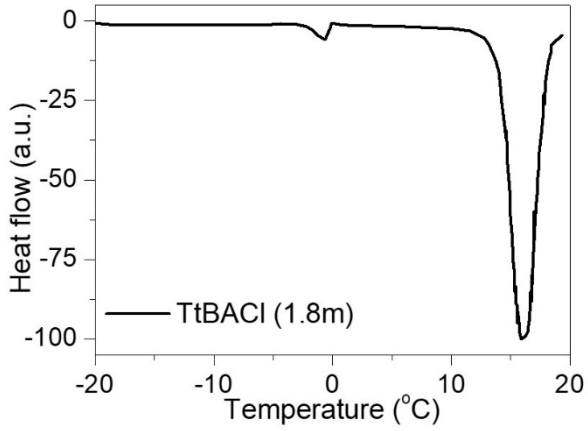

Figure S9. DSC of a 1.8 m solution of tetrabutylammonium chloride (TtBACl), showing the melting of the clathrate and a tiny peak of ice, signaling the presence of a small amount of bulk water.

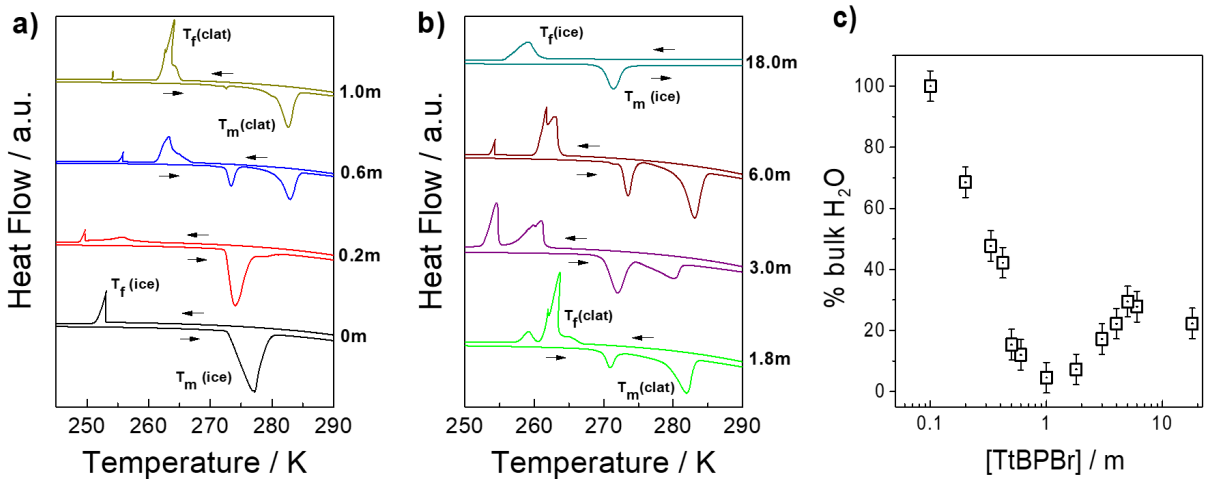

Figure S10. a) and b) DSC scans of pure water and seven solutions with an increasing concentration of tetrabutylphosphonium bromide (TtBPBr). The exo/endothermic peaks at T_f(ice) / T_m(ice) correspond to the formation/melting of ice, and T_f(clat) and T_m(clat) correspond to the formation and melting of the crystalline clathrate hydrates. The large endothermic peak at T_f(ice) was cut to fit in the same scale. c) Fraction of bulk water forming ice extracted from the comparison of the areas of the melting peaks at 273 K of different solutions and pure water. The data show that at ≈1.0-1.5 m most of the water molecules are forming the crystalline lattice of the clathrate structure at low temperature.

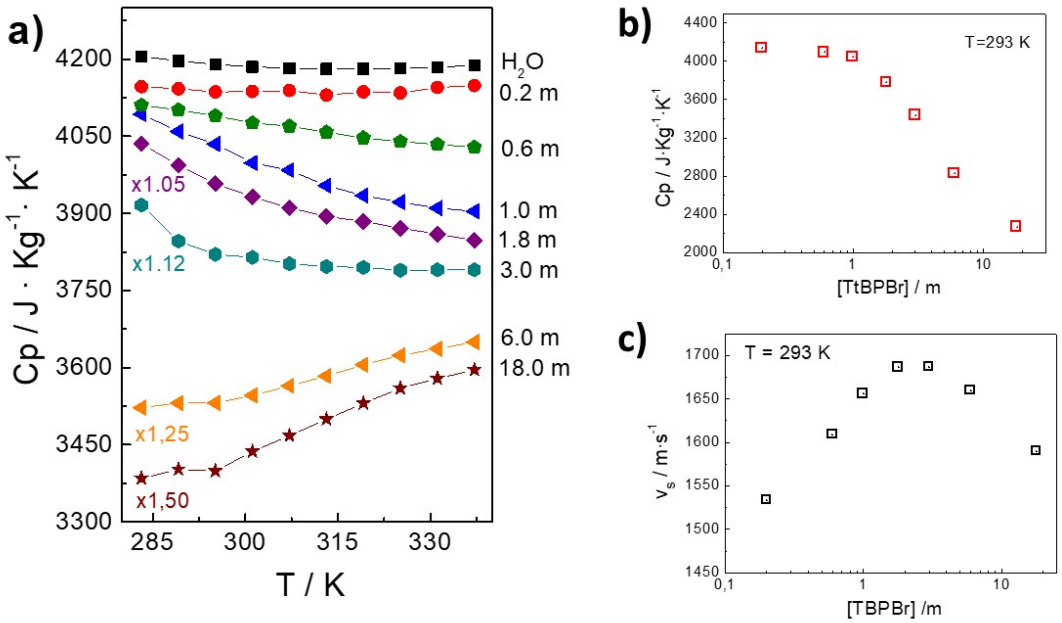

Figure S11. Temperature dependence of the heat capacity (a), and its variation with concentration of different tetrabutyl phosphonium bromide (TtBPBr) solutions at 293 K (b). The sound velocity of different solutions of TtBPBr in water at 293 K is shown in c).

5. Electrochemistry with Cu electrodes.

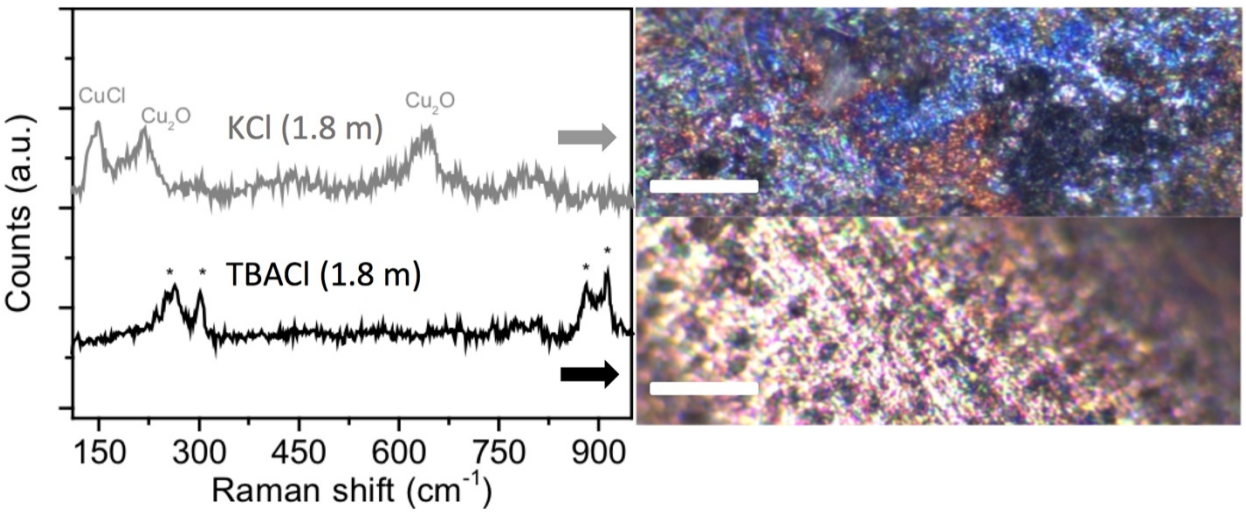

Figure S12. Raman spectra (on the left) and optical images (on the right) of the surface of the Cu electrode used after the experiments reported in section III.2 (chronoamperometry), in a solution of KCl or TtBACl, both 1.8 m. Only the peaks corresponding to the presence of TBA^+ (marked as *) can be clearly observed on the Raman spectrum of the Cu electrode used in the experiment with TtBACl (1.8m) as the electrolyte, however when KCl (1.8m) is used instead, the presence of both CuCl and Cu_2O are observed on the surface of the Cu electrode. The observed peaks are in agreement with the presence of a blue solid film covering the Cu electrode used in the KCl experiment.

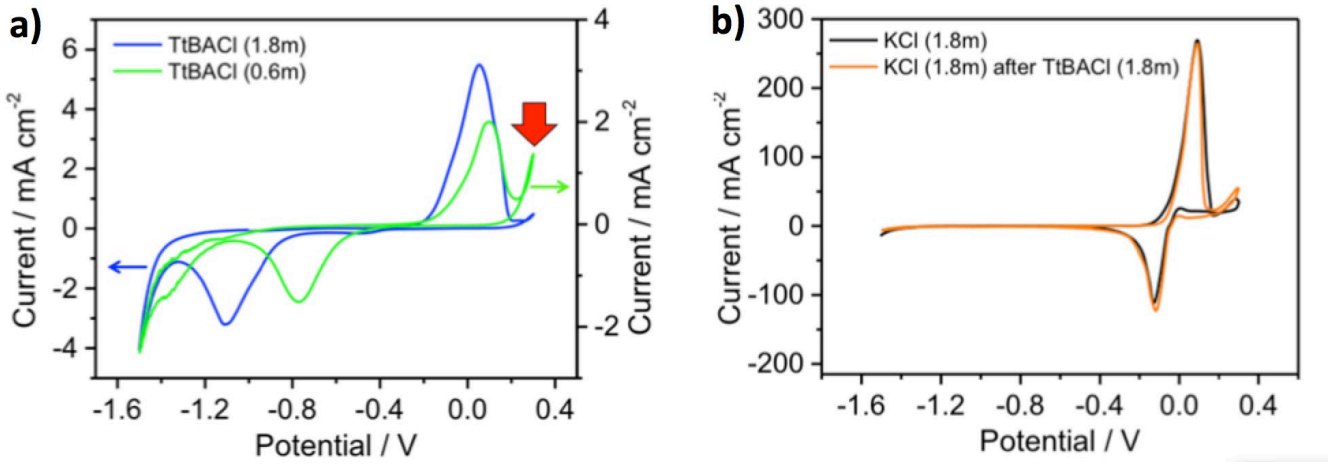

Figure S13. a) Comparison of the cyclic voltammograms of a Cu wire in 1.8m TtBACl (blue) and 0.6m TtBACl (blue) at 50mV/s. b) Comparison of the cyclic voltammogram of a Cu wire in 1.8m KCl with the one done also in 1.8m KCl (orange) but after the electrochemical experiment (Figure 8a) with the clathrate solution (1.8 m) in which the electrode surface was showing the presence of $TtBA^+$ by Raman.